Introduction

Many of the world's continents are bounded, or traversed, by vast fault networks that move laterally, like the well-known San Andreas Fault. These strike-slip regimes are vitally important to the world's natural resources – petroleum, water, and geothermal energy. This book covers all aspects of transform and strike-slip regimes: how they initiate, how they develop, and the natural resources associated with them. Numerous global case studies are utilized to illustrate structural development, thermal and fluid flow implications, and commercial applicability. The work aims to be useful to a broad range of readers, from students of geology and researchers specializing in strike-slip regimes to geoscientists and managers involved in the business of natural resources and energy solutions.

The concept for the book originated with the projects "Petroleum systems of sheared margins" and "Thermal history of transform margins," researched during 2014–2020. Building on earlier regional transform margin projects focused on the Guyana–Suriname Basin, West Australian transform margins, the Coromandal transform of East India, and Equatorial Atlantic transform margins, these two projects examined exploration in strike-slip and transform margin settings, using the large literature base and original research, addressing gaps in knowledge. A key objective of the research was to highlight the differences between transform and extensional rift margins. The combined research on transform margins indicates that exploration practices developed for rifted margins have limitations when applied to transform margins.

This follow-on synthesis brings considerable additional data into the picture, including results of long-term research focused on strike-slip terrains and transform margins, and includes a more extensive database documenting structural styles, thermal regimes, petroleum systems, and rates of geologic processes.

The volume utilizes examples of strike-slip terrains with large databases gathered over decades of research including the Los Angeles and San Joaquin Basins of the San Andreas Transform Fault System, the Central Sumatran Basin associated with the Sumatran Fault, and the Drava, Sava, and Vienna Basins associated with the boundary faults of the ALCAPA terrane in the Carpathians. Classical petroleum provinces of the Los Angeles and San Joaquin Basins in California and Vienna Basin in the Carpathian hinterland indicate that these basins can host several coexisting petroleum systems. In addition, medium- and high-temperature geothermal fields and prospects occur in these strike-slip provinces. Eleven fields in the Salton Sea region are hosted by high-temperature geothermal systems, as well as the Coso field and Medicine Lake prospect further north.

Research into transform margin settings generally lags behind research on rifted margins. However, some transform settings, such as the St. Paul, Romanche, Davie, Guayana, Northern Demerara, and Agulhas–Falkland transform margins, are currently undergoing extensive investigation and developing large databases, all of which are included in this volume.

While the oceanic basins of a transform used to be viewed by hydrocarbon exploration as outboard of the area of interest, current transform margin research brings multiple results indicating the contrary. For example, the South American side of the Romanche and Guyana transform margins borders several distinct ridges and troughs at the oceanic fracture zones, developed during the time when both transforms were in their oceanic–continental development stage. It is becoming evident that these intersections may create unique effects on sediment routing, possible source rock development, heat flow, and migration pathways.

In this book we employ a three-part approach – first addressing the fundamental controls, architecture, and fluid flow characteristics of strike-slip regimes, then moving on to the implications for thermal regimes, and finally considering applicability to petroleum systems.

The first block synthesizes the structural, depositional, erosional, and fluid flow knowledge necessary to understand strike-slip and transform margin settings. It begins with basic descriptions of structural styles and tectonic transport, understanding of which is necessary for the proper layout of geophysical surveys. It includes determination of crust types, which are necessary for definition of different petroleum system candidates; considers structural segmentation, which defines the size and geometry of a potential petroleum system; and addresses structural timing, which is necessary for understanding source/reservoir/trap/seal temporal relations. This block also reviews the kinematics and dynamics of strike-slip faults, the evolution of transforms through the continental, oceanic–continental, and transform margin stages, and the controlling role of lithospheric composition. The block concludes by describing occurrences, mechanisms, rates, and controlling factors of associated fluid flow systems and magmatism.

The second block develops the thermal foundation for geothermal and petroleum system analysis. It evaluates critical factors influencing the thermal history of rocks in strike-slip and transform margin settings, including the effects of pre-rift heat flow regime, lithostratigraphy, deposition, structural framework, erosion, and deformation. It concludes with a description of key elements necessary for an efficient geothermal fluid flow system. It does this by characterizing play concept elements of geothermal fields and prospects worldwide.

The third block investigates implications of the strike-slip and transform margin setting for associated petroleum systems. It systematically describes source rock distribution, maturation and generation history, reservoir distribution, seal distribution, potential migration scenarios, trap types, and preservation issues. Again, a large array of global examples is presented to illustrate these concepts.

1 Basic Description of Structural Architecture in Transform Margin Settings

1.1 Introduction

Throughout this book, we will consider in detail many aspects of strike-slip faults in general, and transform margins in particular. The aim of this introductory chapter is to focus on the classification of the various types of strike-slip faults, and on their structural architecture.

In order to understand structural styles of transform margins, one needs to discuss continental strike-slip fault zones and pull-apart basins, transform margin precursors represented by continental transforms and continent–ocean transforms, and to consider their tectonic development histories, controlling dynamics, and resultant structural architecture. Because transform margins evolve through the continental–oceanic stage, a discussion of ridge transform faults and associated oceanic fracture zones is also required. This overview aids understanding of the structural architecture of the oceanic side of the continental–oceanic transform fault zone, its development history, its controlling dynamics, and the way they affect the evolution of the adjacent continental side, which subsequently evolves into the future transform margin.

1.2 Classification of Strike-Slip Faults

Strike-slip faults are faults with the dominant component of the slip vector being parallel to the fault strike (Le Pichon et al., 1973; Bates and Jackson, 1987). Serving as more-or-less restraining structures, continental strike-slip faults have a geometry related to the controlling stress field; that is, their structural architecture is controlled by the evolving hosting mechanical stratigraphy and local stresses (e.g., Gerya, 2016).

Strike-slip fault classification represents a problem, because the continental examples do not function as steady-state features (e.g., Gerya, 2016). Instead, they progressively evolve, and adjust their location and geometry with time (e.g., Norris and Toy, 2014). As discussed in Chapter 5, on top of changing their tectonic position and geometry, strike-slip faults can progressively increase their lateral and vertical extent to the point where they involve lithospheric layers other than the one where they nucleated. This is the main reason why most older classifications, which divide strike-slip faults based on their extent, do not work very well, classifying strike-slip faults based on snapshots and not on their entire development history.

If we want to use currently available strike-slip classifications (e.g., Wilson, 1965; Sylvester, 1988; Twiss and Moores, 1992), we can try to edit them with the understanding that some of their categories do not necessarily describe fully mature strike-slip faults but their earlier evolutionary stages. For example, based on their interplate versus intraplate extents, strike-slip faults can be divided into transform faults (Wilson, 1965), which are cut through the entire lithosphere in their fully developed stage, and transcurrent faults, which remain inside the lithosphere even in their fully mature stage (Sylvester, 1988; Table 1.1; Figure 1.1). This approach will ensure that the classification we use honors a relatively new understanding that the structural architecture of continental transforms develops gradually, and that these faults tend to utilize preexisting lithospheric anisotropy during their propagation (Norris and Toy, 2014). This approach will also honor the new concept (see Gerya, 2010, 2013a, 2016) that the spontaneous development of ridge transforms in numerous spreading systems needs a several-million-year time period of gradual development to reach a steady state.

Even such an edited classification is still problematic, because continental transforms and some oceanic transforms have controlling dynamics, development history, and structural architecture different from each other. Therefore, before we discuss characteristic features of individual strike-slip fault categories and typical natural examples of these (Table 1.1), we need to look at these differences.

Table 1.1 Strike-slip fault classification (modified from Wilson, 1965; Bally, 1982; Bosworth, 1985; Rosendahl et al., 1986; Woodcock, 1986; Mascle and Blarez, 1987; Rosendahl, 1987; Sylvester, 1988; Versfelt and Rosendahl, 1989; Morley et al., 1990; Ratschbacher et al., 1991a; Twiss and Moores, 1992; Detrick et al., 1993; Younes and McClay, 2002; Destro et al., 2003; Bonatti et al., 2005; Govers and Wortel, 2005; Sclater et al., 2005; Escalona and Mann, 2006; Nemčok et al., 2006a; Gregg et al., 2007, 2009; Roland et al., 2010; Ben-Avraham et al., 2012; Géli et al., 2014; Maia et al., 2016; Morrow et al., 2016; Kolandaivelu et al., 2017; Burg, 2018).

Transform faults (cut through entire lithosphere, in some cases at least in their fully developed stage)	
Transform faults linking ridge with ridge (Figures 1.1, 1.2a)	Relatively dynamically stable transforms that displace segments of oceanic lithosphere accreted under similar spreading vectors and most likely different spreading rates (the term oceanic fracture zones describes their two inactive portions beyond the transform intersections with neighbor ridges) Present-day active examples: Atlantis, Charlie Gibbs, Hayes, Kane, Oceanographer, Pico and Vema transforms, slow-spreading Mid-Atlantic Ridge region Clarion, Discovery, Garrett, Gofar, Orozco, Quebrada and Siqueiros transforms, fast-spreading East Pacific Ridge region Blanco transform separating Juan de Fuca and Gorda ridges, offshore Oregon Large-offset Romanche and St. Paul slowly slipping transforms of the Equatorial Atlantic Andrew Bain, Du Toit, Marion and Prince Edward transforms, slow Southwest Indian Ridge region Menard transform, Pacific-Antarctic Ridge region Guamblin transform, Chile Rise Ecuador transform separating Costa Rica and Ecuador rifts
Transforms evolved from the continental transform stage, through the oceanic–continent transform stage, into the transform margin stage (Figures 1.1, 1.6a)	Transforms that cut through the continental lithosphere linking two nucleated spreading centers, which subsequently evolve to oceanic–continental transforms as two continental blocks clear each other and continental sides are juxtaposed with laterally passing oceanic crust and its associated spreading center. Their subsequent inactive portions are transform margins juxtaposed with progressively cooling oceanic lithosphere. Examples: Romanche (Figure 1.6b) and St. Paul transforms of the Equatorial Atlantic that underwent their ocean–continent stages during the Albian–Campanian and Albian–Cenomanian, respectively Zenith–Wallaby–Perth and Cape Range transforms in West Australia that underwent their ocean–continent stages during the Barremian–Albian and Valanginian–Barremian, respectively
Transforms linking ridges with convergent plate boundary (Figures 1.1, 1.7a). The two subtypes of this category include transforms that link the ridge with overriding versus subducting plates of the subduction zone.	Transforms with tendency to change their length Examples: the eastern portion of the northern boundary of the Caribbean Plate; i.e., transform fault zone linking the spreading center in the Cayman Trough with the accretionary wedge at the eastern front of the Caribbean Plate (Figure 1.8a) The San Andreas Transform linking the subduction zone, where the North American Plate overrides the Pacific Plate, with a system of spreading centers in the Gulf of California (Figure 1.7a) The Dead Sea Transform linking the spreading ridges of the Red Sea with the overridden plate of the Arabia–Eurasia collisional zone (Figure 1.12) The Sagaing Transform linking the spreading center of the central Andaman Basin with the overridden plate of the India–Eurasia collisional zone (Figure 1.9) The Queen Charlotte Transform linking the spreading ridge with the subducting plate of the subduction zone

Table 1.1 (cont.)

Transforms linking convergent plate boundaries (Figure 1.2a). The two subtypes of this category include transform faults that link either two overriding or overridden plates. The third subtype includes a linkage of the overriding one with overridden one. Further combinations arise when we divide convergence zones into subduction and collision zones.	Transforms with tendency to change their length Examples: the Alpine Transform in New Zealand, linking a combination of overriding and overridden plates The fault system forming the southern boundary of the Caribbean Plate, linking the overriding Caribbean Plate of the subduction zone with the overriding plate of the Nazca–South America subduction zone (Figure 1.8a) The Chaman Transform linking a combination of the overriding Eurasian Plate with the Makran Range and overridden Indian Plate of the India–Eurasia collisional zone (Figure 1.12) The North Anatolian Fault linking the overriding plate of the Arabia–Eurasia collision zone with the overriding plate of the Hellenic subduction zone (Figure 1.12) The East Anatolian Fault linking the overriding plate of the Arabia–Eurasia collision zone with the overriding plate of the Anatolia–Africa subduction zone (Figure 1.12)
Trench-linked strike-slip faults (Figure 1.1)	Strike-slip faults that accommodate the horizontal component of oblique subduction Examples: Atacama Fault, Chile, South Japan Sea Fault Zone and Median Tectonic Line, Japan, Sumatran Fault (Figure 1.9)
Transcurrent faults (reside inside lithosphere even in their fully developed stage)	
Indent- and lateral extrusion-linked strike-slip faults (Figure 1.1)	Strike-slip faults that separate continental blocks that move with respect to each other in the convergent plate setting Examples: Red River Fault, Steinberg Faults and Farské, Schrattenberg-Bulhary, and Central Hungarian Fault zones in the Western Carpathian–Pannonian region (Figure 1.10), Moesian Platform Faults in front of the Carpathians (Figure 1.11)
Transfer faults	Strike-slip faults that transfer horizontal slip component from one set of faults to another set of faults. They include: accommodation zones, transfer zones and interference accommodation zones Examples: Jeremboabo Fault in the Jatobá–Tucano–Reconcavo Rift Zone, NE Brazil, Rukwa Transfer Zone between Malavi and Tanganyika Rift Zones, East African Rift System The Garlock Fault separating the Central Basin and Range Province with the larger amount of extension and the Mojave Block with the smaller amount of extension Kala Bagh and Jhelum faults bounding the Potwar Plateau on its east and west sides (Figure 1.15a), Pakistan Faults along the east and west sides of the Sulaiman Range, Pakistan (Figure 1.15b)
Tear faults	Strike-slip faults that accommodate differential displacement within a specific allochthon or between allochthon and its adjacent structural units Examples: Jacksboro and Russell Fork Faults bounding the Pine Mountain thrust sheet from SW and NE, respectively, in the Appalachians A dense system of tear faults deforming the frontal portion of the northern Variscan orogenic belt in Southern Wales, UK (Figure 1.16a)
Small-scale conjugate strike-slip fault systems in individual thrust sheets	Strike-slip faults with a role to accommodate for the coeval strike-parallel stretching and orthogonal shortening. Examples: small-scale conjugate strike-slip faults in individual frontal anticlines of thrust sheets in the Eastern Carpathians, Romania, Makran and Sulaiman Ranges (Figure 1.17), Pakistan, Jura fold and thrust belt, Switzerland

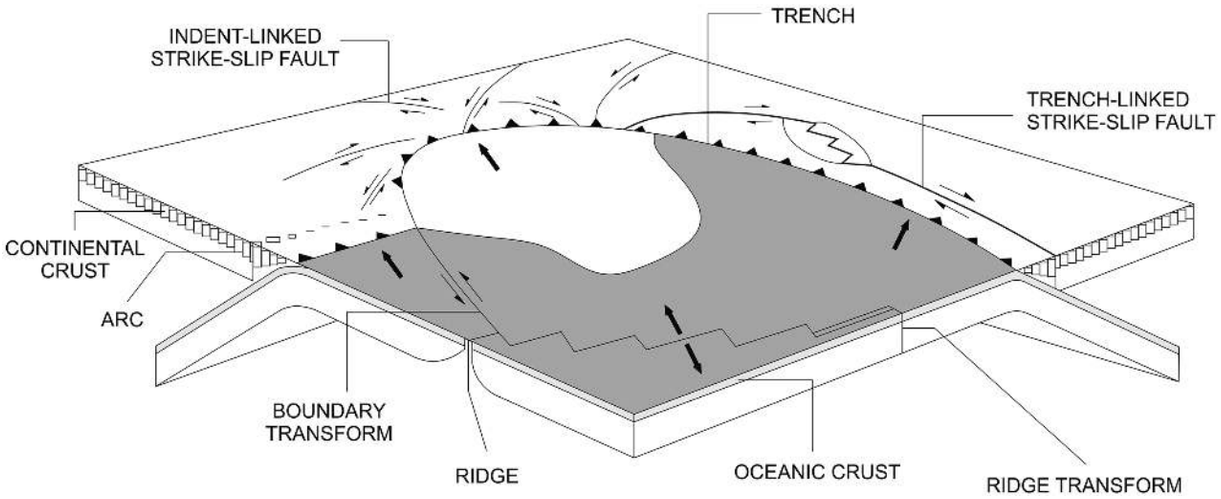

Figure 1.1 Schematic diagram showing different types of strike-slip faults (Woodcock and Fischer, 1986).
Reprinted from the *Journal of Structural Geology*, 8, Woodcock, N. H. and Fischer, M., Strike-slip duplexes, 725–735. ©1986, with permission from Elsevier.

While continental transforms are plate deformation structures (see Norris and Toy, 2014 and references therein), transforms linking spreading ridges in intermediate, fast, and some slow spreading systems are plate growth structures once they reach their steady-state development (Gerya, 2012, 2013a).

The structural architecture of continental transforms develops gradually and tends to utilize pre-existing lithospheric anisotropy during transform propagation (Norris and Toy, 2014). Plate boundary localization in the case of continental transforms requires a significant perturbation of composition, stress, or temperature in the lithosphere or the underlying asthenosphere (Molnar and Dayern, 2010; Burov and Gerya, 2014). Evidence from numerous continental transforms discussed in Chapter 5 indicates that all of them started their development as broad deformation zones, where a dominant fault zone developed subsequently (e.g., Atwater, 1970; Şengör, 1979; Sutherland, 1995; Yue and Liou, 1999; Norris and Toy, 2014). They try to establish Andersonian geometry with respect to their controlling stress field (see Anderson, 1951), but deviation from the Andersonian geometry is caused by both the effect of pre-existing zones of weakness (e.g., Wallace, 1951), as discussed in Chapter 6, and adjustment to the required plate boundary geometry.

Observations and modeled scenarios indicate that oceanic transforms in ultra-fast, fast, intermediate-fast, and some slow spreading systems in their mature stages are not plate deformation structures like continental transforms. Rather, they are plate growth structures (Gerya, 2010, 2013a, 2016). They serve as lubricants for displacement of segmented plates undergoing coeval divergence and accretion. They do not have Andersonian geometry (Anderson, 1951) with respect to their controlling stress field. Instead, they are parallel to the σ_3 direction. They represent features promoted by dynamic instability controlled by the asymmetric lithospheric accretion enabled by strain-weakening faults (Gerya, 2010). This instability is most distinct in model runs at spreading rates of 38–57 mmy^{-1}, which is in accordance with observations of orthogonal transform patterns less typical for spreading systems that are faster and slower than this range of spreading rates (e.g., Naar and Hey, 1989; Dick et al., 2003; Kriner et al., 2006; Gerya, 2010; Puthe and Gerya, 2014).

While transform seismicity is characterized by magnitudes smaller than those of subduction and collision settings (Gerya, 2016), there is a difference between continental and oceanic transforms.

Continental transforms are characterized by more-or-less diffuse active faulting and, frequently, only a fraction of the plate displacement is accommodated by seismoactive faulting (e.g., Sibson, 1983; Field et al., 2009; Carpenter et al., 2011). The San Andreas Fault, for example, indicates a phyllosilicate-rich foliated and fluid-saturated fault core, which is considerably weaker than the host rock and is unable to frictionally heal (e.g., Moore and Rymer, 2007; Collettini et al., 2009), controls fault displacement by aseismic creep along most of its segments (Carpenter et al., 2011). Seismoactive faults of continental transforms are not continuous, but are divided into segments separated by step-like discontinuities (Wesnousky, 2006).

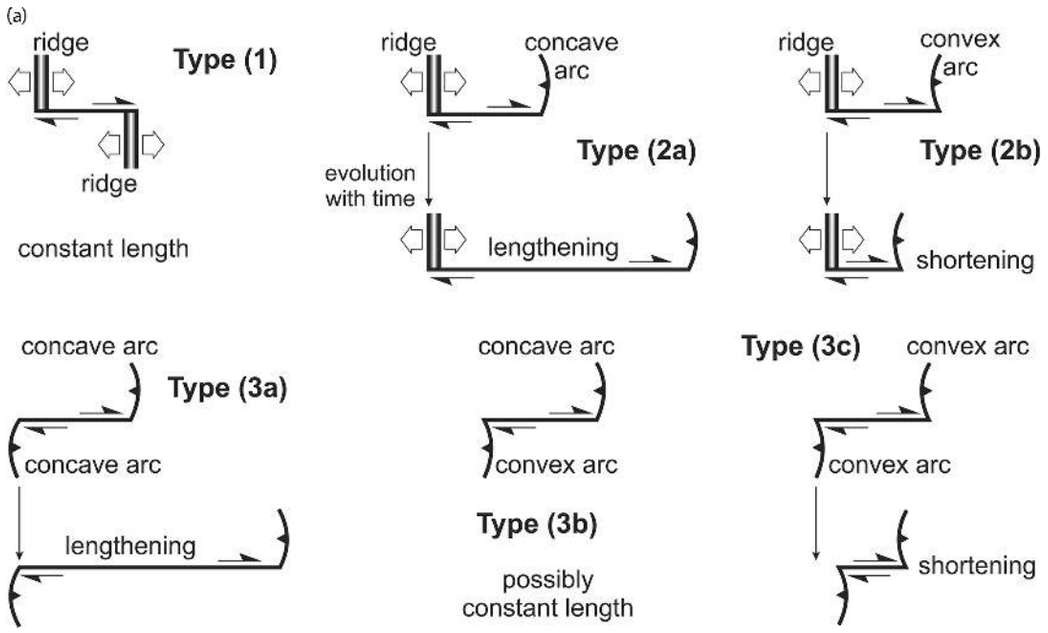

Figure 1.2 (a) Basic types of transforms based on the possible configurations of neighbor plate boundaries (Wilson, 1965). Reprinted by permission from Springer Nature: *Nature*. Wilson, J. T. A new class of faults and their bearing on continental drift. 207, 343–347. ©1965.

Oceanic transforms are characterized by more-or-less concentrated faulting and most of the plate displacement is accommodated by aseismic creep (Brune, 1968; Davies and Brune, 1971; Kanamori and Stewart, 1976; Frohlich and Apperson, 1992; Okal and Stewart, 1992; Okal and Langenhorst, 2000; Bird et al., 2002; Boettcher and Jordan, 2004). Mature oceanic transforms are distinctively weak (Gerya, 2010, 2013a; Allken et al., 2012). The weakness is interpreted to be caused by deep hydration and serpentinization (e.g., Escartín et al., 2001; Hilairet et al., 2007; Korenaga, 2007). Faults composing the oceanic transform tend to be linear and their earthquake magnitudes are small (Gerya, 2016). The few larger magnitudes characterize either new transform propagation (e.g., Delescluse et al., 2012; McGuire and Beroza, 2012) or the reactivation of oceanic fracture zones (Robinson, 2011) in some cases.

1.3 Interplate Strike-Slip Faults

1.3.1 Transform Faults Linking Ridge with Ridge

This type of transform (Figure 1.2a) separates blocks of oceanic lithosphere in intermediate and some fast and some slow spreading systems, where the described spreading rate categories are using criteria from Small (1998), Dick et al. (2003), and Kriner et al. (2006). The structural architecture in this case can be characterized as an orthogonal pattern of transforms (e.g., Freund and Merzer, 1976; Figures 1.2b, 3.2a, and 3.2e; S3 architecture in Figure 1.2c). This pattern evolves in the following different lithospheric settings:

1) some slow spreading systems that develop a new oceanic lithosphere by magma-assisted spreading; and
2) intermediate and fast systems that develop a new oceanic lithosphere by magma-assisted spreading.

It needs to be emphasized that the structural architecture is rather different in spreading systems that are either faster or slower than the aforementioned systems (Figure 1.2c). For example, observations and modeling indicate that ultra-slow and some slow spreading systems do not develop well-pronounced transforms, but rather curved spreading centers (Shemenda and Grocholsky, 1994) or oblique amagmatic spreading sections (Dick et al., 2003; Puthe and Gerya, 2014) instead of transforms (S1 architecture in Figure 1.2c). Oblique shear zones were described, for example, from some segments of the slow spreading Mid-Atlantic Ridge (Schouten and White, 1980; Sempere et al., 1993). This tectonic setting evolves in pre-existing lithosphere affected by stretching.

In the case of some modeled fast spreading systems, transforms are initially possible but do not represent a

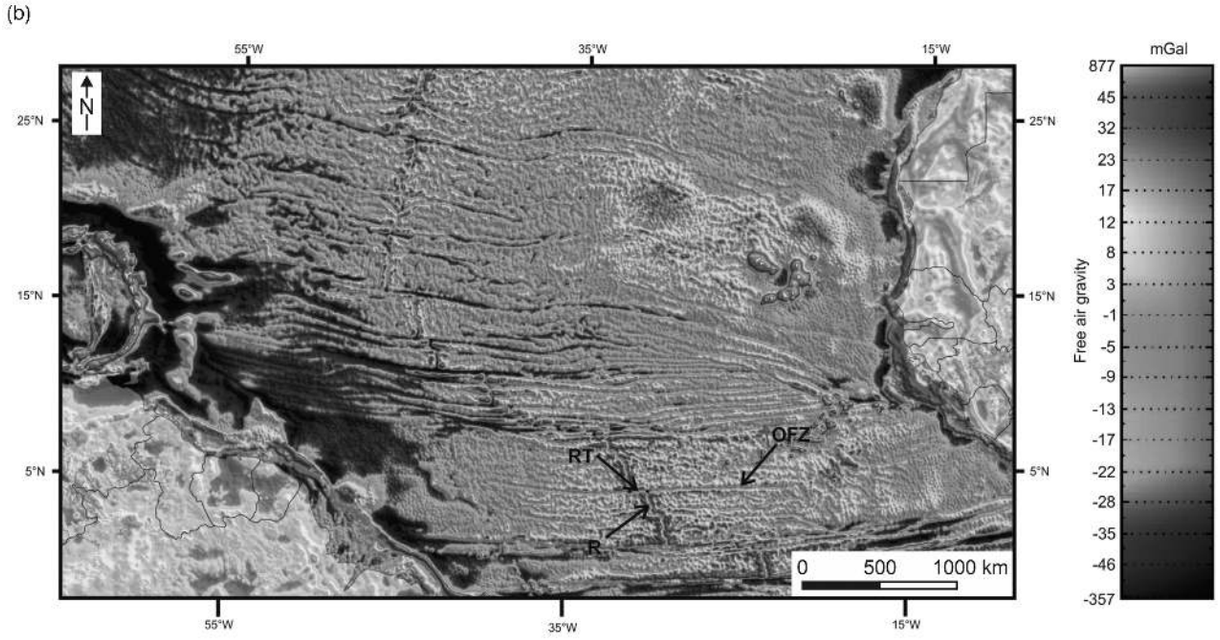

Figure 1.2 (b) Free-air gravity anomaly map of the southern Central Atlantic and western Equatorial Atlantic imaging a system of Mid-Atlantic Ridge segments and linking ridge transforms (modified from Nemčok et al., 2015a). Abbreviations: OFZ – oceanic fracture zone, R – spreading ridge segment, RT – ridge transform.

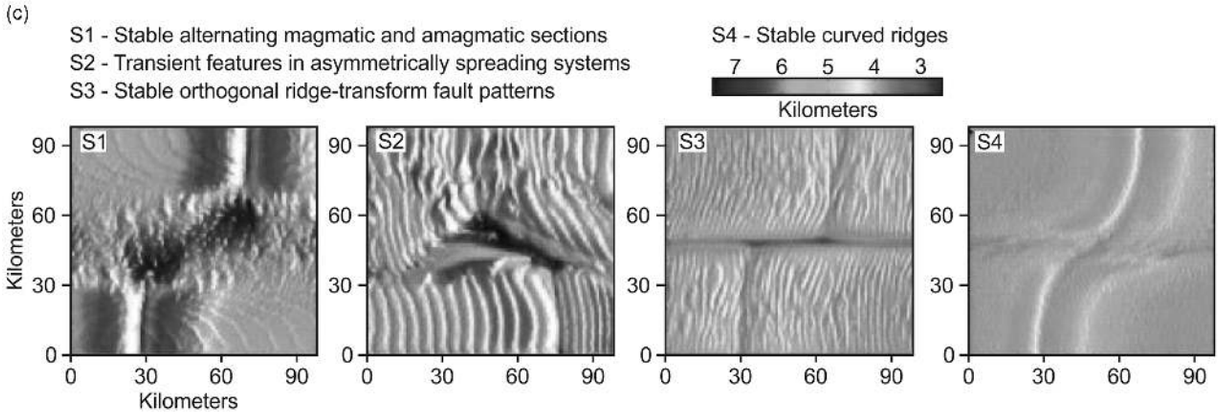

Figure 1.2 (c) Dependence of structural architecture of the spreading system on the spreading rate as indicated by numerical modeling (Puthe and Gerya, 2014). Architectures S1, S2, S3, and S4 represent rates of 10 mmy^{-1}, 20 mmy^{-1}, 40 mmy^{-1}, and 80 mmy^{-1}, respectively. See text for further explanation.
Reprinted from *Gondwana Research*, 25. Puthe, C. and Gerya, T. Dependence of mid-ocean ridge morphology on spreading rate in numerical 3-D models. 270–283. ©2014, with permission from Elsevier.

steady-state feature, because they become replaced by curved ridge sections after a few million years (Gerya, 2016; S4 architecture in Figure 1.2c). Furthermore, the models of ultra-fast systems are characterized by the absence of transforms at rates exceeding 140 mmy^{-1} (Naar and Hey, 1989; Kriner et al., 2006). Ridge offsets are accommodated by microplates, propagating rifts, and overlapping spreading centers (Kriner et al., 2006). Overlapping centers are described, for example, from some segments of the fast spreading East Pacific Rise (Macdonald and Fox, 1983; Lonsdale, 1985). Both fast and ultra-fast systems evolve in magma-assisted crust and lithospheric mantle affected by dominating buoyancy forces and subordinate stretching.

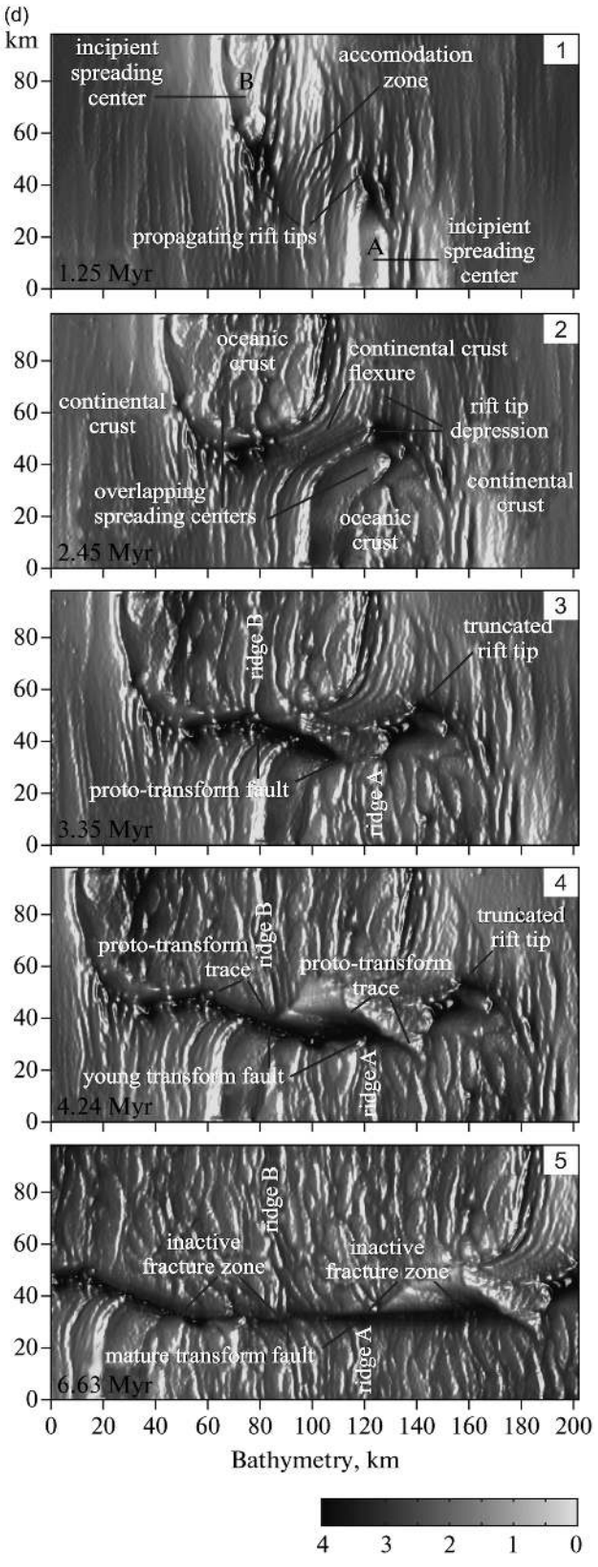

The aforementioned non-transform discontinuities from both very slow and very fast spreading systems can be characterized as follows. Those not exceeding a length of a few tens of kilometers are short-lived and known to be able to migrate along the strike of the spreading system (Macdonald et al., 1991). The longer ones are more stable, able to last several million years. Unlike ridge transforms, their outboard extensions do not form small circles reflecting the pole of relative motion (Detrick et al., 1993).

A steady-state transform representing intermediate, some fast and some slow spreading systems is composed of a zone of distinct troughs and ridges, which can be more than several tens of kilometers wide (Figures 3.5c, 3.13a–c, 3.16, and 7.23). Their elevation difference from the top of the undeformed oceanic crust can reach several kilometers (Figures 3.13a, 3.13c, 7.23). Individual strike-slip faults of the transform represent a narrow fault zone along which oceanic plate segments are passing each other horizontally (Detrick et al., 1993). It is relatively stable for millions of years. Ridge transform faults of intermediate, fast and some slow spreading systems are commonly perpendicular to the spreading ridge segments and parallel to the spreading–controlling extension (Oldenburg and Brune, 1972; Gerya, 2016; Figure 1.1) once they reach the steady-state development (Figure 1.2d). They play an important role in affecting the thermal regime, mantle flow, melting, and crystallization at mid-oceanic ridges (Fox and Gallo, 1984; Parmentier and Forsyth, 1985; Phipps Morgan and Forsyth, 1988). Active, ridge-connecting transforms, which are usually tens to hundreds of kilometers long, extend further out from between the spreading ridges as inactive oceanic fracture zones of similar geometry (Detrick et al., 1993; Gregg et al., 2007; Figures 1.2b and 1.3). These extensions, represented either by zones of weakness or locked fault systems, can be occasionally reactivated in cases of spreading vector and rate changes, and main plate motion changes (Gomes et al., 2000; Robinson, 2011).

Figure 1.2 (d) Numerically simulated development of the ridge transform fault (Gerya, 2013a), representing (1) propagating spreading centers reaching each other, (2) overlapping centers, (3) proto-transform development stage, (4) transform nucleation stage, and (5) transform growth stage. Republished with permission of Springer Nature from Initiation of transform faults at rifted continental margins: 3D petrological–thermomechanical modeling and comparison to the Woodlark Basin. Gerya, T., *Petrology*, 21(6), 550–560. ©2013. Permission conveyed through Copyright Clearance Center, Inc.

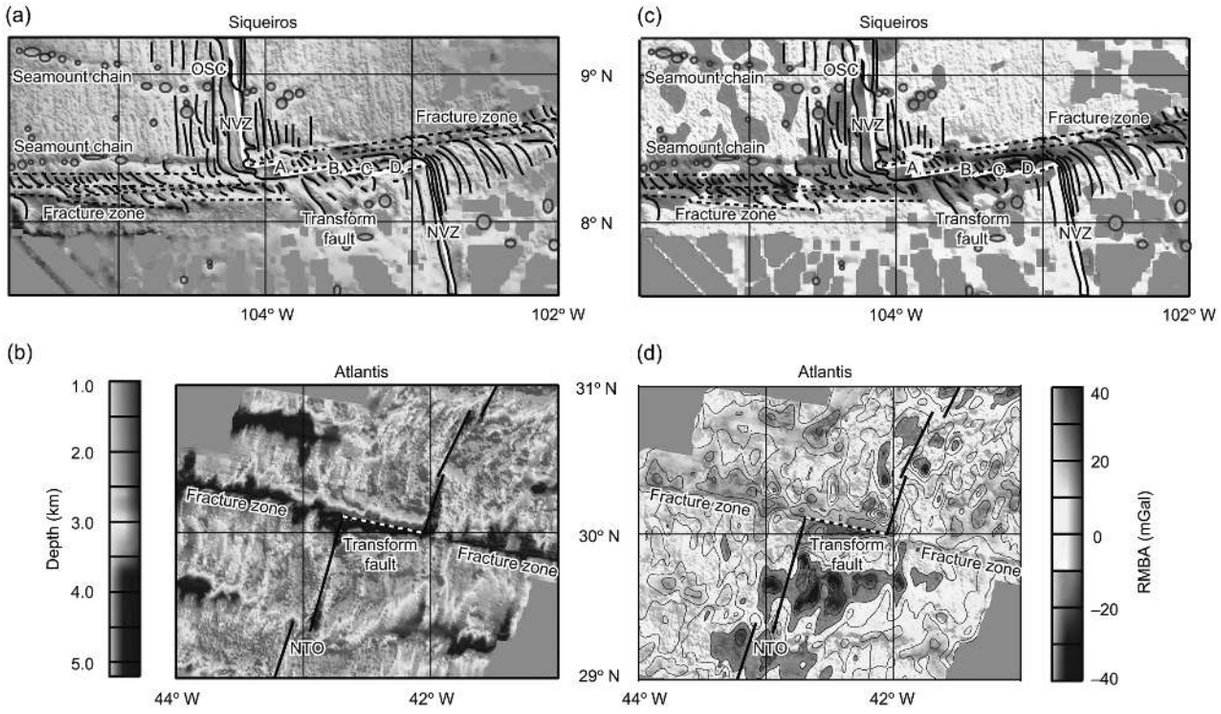

Figure 1.3 Bathymetric and residual mantle Bouguer anomaly maps of fast slipping Siqueiros and slow slipping Atlantis ridge transforms (Gregg et al., 2007). (a) Bathymetric map of the Siqueiros Transform. Solid black lines – structural architecture of oceanic crust, dashed black lines – transform and oceanic fracture zone locations, circles – seamount locations, white line – plate boundary. NVZ – neo-volcanic zone, OSC – overlapping spreading center. (b) Bathymetric map of the Atlantis Transform. Black and white lines indicate transform and spreading centers. NTO – non-transform offset. (c) Residual mantle Bouguer anomaly map of the Siqueiros Transform. (d) Residual mantle Bouguer anomaly map of the Atlantis Transform.

Furthermore, because the thermal contraction continues as the oceanic lithosphere drifts away from the spreading ridge, some dip-slip displacement can be expected along oceanic fracture zones. In these cases, the older lithosphere forms the hanging wall. In most cases oceanic fracture zones are aseismic. They can be traced for thousands of kilometers (Figure 1.2b) onto the ridge flanks as small circles reflecting both the direction of plate motion and the divergence of plates on either side of the ridge, as a function of rotation around an Euler Pole (Menard and Chase, 1970).

In contrast to continental strike-slip faults, the ridge transforms may show opposite displacement sense within a pattern characterized by the same strike. Furthermore, the displacement sense of the ridge transform can be opposite to what is apparent from the spreading ridge offset.

The thermal regime and mechanical behavior of ridge transforms are distinctively different from those of continental transforms. This is due to heat conduction and advection from the warmer, younger plate into the older, colder plate (Louden and Forsyth, 1976; Roland et al., 2010; Kolandaivelu et al., 2017) and the elastic layer development, which both cause ridge transforms to have unusual topographic and gravimetric structure (Sandwell and Schubert, 1982; Sandwell, 1984; Pockalny et al., 1996).

As documented by submersible studies of the Oceanographer and Vema ridge transforms (OTTER Scientific Team, 1985; Auzende et al., 1989), the walls of both transform faults and their oceanic fracture zones represent steep outcrops of basaltic, gabbroic, and ultramafic rocks. Furthermore, the crustal architecture of ridge transform faults and their oceanic fracture zones differ from that of normal oceanic crust (Detrick et al., 1993, and references therein). Slow slipping Atlantic Transforms and their fracture zones cut the oceanic crust, which is thinner than normal (Figure 1.4). Mantle Bouguer anomaly images of these transforms are represented by anomalies that are more